Review of Microcrack Detection Techniques for Silicon Solar Cells

Mahmoud Abdelhamid, *Student Member, IEEE*, Rajendra Singh, *Fellow, IEEE*, and Mohammed Omar

***Abstract*—Microcracks at the device level in bulk solar cells are the current subject of substantial research by the photovoltaic (PV) industry. This review paper addresses nondestructive testing techniques that are used to detect microfacial and subfacial cracks. In this paper, we mainly focused on mono- and polycrystalline silicon PV devices and the root causes of the cracks in solar cells are described. We have categorized these cracks based on size and location in the wafer. The impact of the microcracks on electrical and mechanical performance of silicon solar cells is reviewed. For the first time, we have used the multi-attribute decision-making method to evaluate the different inspection tools that are available on the market. The decision-making tool is based on the analytical hierarchy process and our approach enables the ranking of the inspection tools for PV production stages, which have conflicting objectives and multi-attribute constraints.**

***Index Terms*—Analytical hierarchy process (AHP), crack detection, defects, microcracks, nondestructive testing (NDT), photovoltaic (PV) devices.**

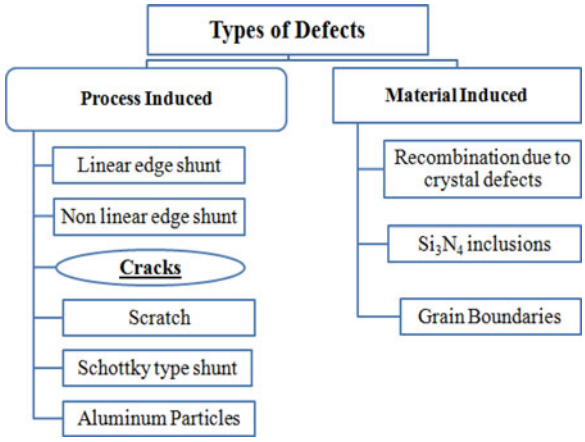

Fig. 1. Some types of cell defects in wafer-based silicon solar cells.

I. Introduction

GLOBALLY, the cumulative installed solar photovoltaic (PV) capacity has topped the 100-GW milestone [1]. Current growth in PV is not confined to any one region of the globe, however, but rather distributed worldwide [2]. As compared with the 35 GW markets of 2013, the PV market with a value of US$155.5 billion is projected to grow to 61.7 GW by the year 2018 [3]. The past success of the PV industry indicates that, for sustained global economic growth, PV offers a unique opportunity to solve the 21st century's electricity generation problem because solar energy is essentially unlimited and PV systems can provide electricity to rich and poor alike [4]. The average selling price of PV panels has dropped to US$0.65/Wp [5]. Silicon-based solar cells have dominated the PV market and account for about 90% of the PV market. For example, in 2012, silicon bulk PV module shipments represented 89% of total amount of 31.3 GW, while thin films (CdTe, CuInSe/CuInGaSe, and a-Si) solar cells contributed to the remaining 11% [6]. Dominated by the second-most abundant element in the earth's crust [7], the PV industry is based mostly on mono- and polycrystalline silicon solar cells and is firmly moving toward the terawatt scale [8]. The highest efficiencies of silicon solar cells and silicon PV modules are 25% [9] and 21.5% [10], respectively. Researchers have been investigating the possible solutions to reducing the gap between the efficiency of a silicon solar cell and that of the PV module. One possibility entails eliminating the shunts, which are internal short circuits where localized current significantly exceeds the homogenously flowing current. Other solutions consider reducing defects that affect the quality of the solar cell or reducing the energy conversion efficiency of the PV module. Fig. 1 shows some examples of the defects in solar cells [11]–[20], categorized as either process induced or material induced.

In this paper, we have focused solely on defects caused by microcracks because wafer breakage decreases the optimal utilization of the production line and leads to the waste of costly production material. The losses that result from microcrack defects can be as high as 5%–10% in a typical manufacturing facility [21]. According to 2011 production costs and wafer prices, a 1% wafer breakage rate costs about US$656 700 annually for an 80 MW production line [22]. Cracked solar cells lead to the loss of yield in manufacturing production line with a consequent increase in production costs. Microcrack defects not only reduce cell efficiency in the field but also reduce cell reliability. Because of the economic importance of microcrack defects, we have reviewed the current inspection techniques used to detect micro crack defects. Though Israil and co-workers [23] have published a review of micro crack detection methods, it has a limited technical scope. Specifically, they did not: 1) address other types of defects that are related to the origin of cracks; 2) classify cracks; 3) engage in a fundamental comparison between various methods; 4) explain all methods for crack detection; and 5) most

Manuscript received July 1, 2013; revised August 16, 2013 and October 2, 2013; accepted October 3, 2013. Date of publication October 25, 2013; date of current version December 16, 2013.

M. Abdelhamid and M. Omar are with the Clemson University International Center for Automotive Research, Greenville, SC 29607 USA (e-mail: mabdelh@g.clemson.edu; MOMAR@clemson.edu).

R. Singh is with the Department of Electrical and Computer Engineering, Clemson University, Clemson, SC 29634-0915 USA (e-mail: srajend@clemson.edu).

Color versions of one or more of the figures in this paper are available online at http://ieeexplore.ieee.org.

Digital Object Identifier 10.1109/JPHOTOV.2013.2285622

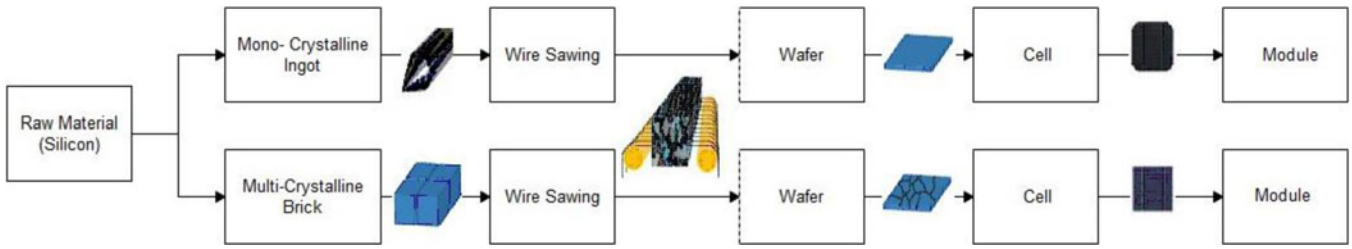

Fig. 2. Key processing steps used in manufacturing of crystalline and poly silicon PV modules.

importantly, provide a description of a method to select the best tool for microcrack detection.

In this paper, we have reviewed following six integral aspects regarding microcracks: 1) as part of the defects of silicon wafers; 2) their origins; 3) their root causes; 4) their full impacts in terms of electrical and mechanical issues; 5) their classification; and 6) the suitable methods used to detect various types of microcracks. For the first time, we have used multi-attribute decision-making tools using the analytical hierarchy process (AHP) to assist in the evaluation and selection of currently available inspection tools that are used for microcrack detection.

In Section II, we discuss the origin and root causes of microcracks followed by the classification of cracks in Section III. The impact of the microcracks on the mechanical and electrical properties of solar cells is discussed in Section IV. A survey of the main techniques used to detect the microcracks is presented in Section V. The advantages and disadvantages of various nondestructive testing (NDT) techniques are discussed in Section VI. The approach that is used to select inspection tools is discussed in Section VII and we sum up our conclusions in Section VIII.

II. Origin and Root Causes of Microcracks

The silicon atoms in a crystalline silicon solar cell are arranged in a diamond lattice unit cell with a lattice constant equal to 0.534 nm. The diamond-crystal lattice is characterized by four co-valently bonded atoms. The fracture in PV cells occurs when the energy available for crack enlargement is sufficient to overcome the resistance of the material. The typical thickness of silicon wafers used for solar cell applications is around 180 μm. These wafers are also quite fragile in that the silicon material used in their construction is most brittle at room temperature, and is characterized by two principle plains of cleavage: $\{1\ 1\ 1\}$ and $\{1\ 1\ 0\}$ [24]–[26]. In various studies undertaken to observe the direction of crack propagation in this material, the preferred propagation direction was in the $<1\ 1\ 0>$ direction on both planes [25].

The cleavage plane $\{1\ 1\ 1\}$ is the easier plane in which a crack may propagate as it has the lowest energy and the lowest fracture energy, which for this plane, is reported as 2.2 J/m^2. The energy needed to fracture silicon material with defects is even lower [26], [27]. In both poly- and single crystalline silicon solar cells, crack propagation in the direction of depth of the wafer typically either terminates or is strongly reduced at the interface between the silicon layer and back contact layer of Al because Al–Si eutectic layer has high fracture toughness [28], [29].

The thermal stress that is generated during various thermal processing steps is the main cause of microcracking. Fig. 2 shows the main processing steps used in the manufacturing of crystalline and polysilicon PV modules. The feedstock is melted at high temperatures. Overly long melting and holding periods combined with the high temperatures prior to crystallization can lead to higher impurity transfer between the ingot and crucible. During the block sawing stage, the produced heat can cause thermally induced stress, which in addition to the sawing forces, can cause the initiation and propagation of cracks, most particularly from the saw damages to the block [30]. Microcracks are usually introduced at the wire sawing stage of blocks/ingots [31]. If the cracked wafers are processed as normal wafers, more cracks occur introduced during the thermal processing steps used in the cell production. The biggest challenge is the detection of microcracks that are generated during this sawing process, since these defects are hidden within the bulk of the wafer.

Saw-damage etching, which is a procedure performed in order to remove the surface damage caused by wire sawing, is another production process that causes microcracking [32]. Different methods for chemical etching and texturing are used in solar cell manufacturing. In their study of the effect of saw-damage etching on microcracks, Larsson *et al.* [33] reported that neither alkaline nor acidic saw-damage etching increased the microcracks length, but did decrease the shallow parts of the cracks since the surrounding silicon is etched away. If the initial crack is large enough, the crack can widen and deepen after etching, possibly by etching the edges of the fracture.

The etching time, and consequently, the etching depth is a major process parameter influencing the mechanical stability of the wafer [34], [35]. Schneider *et al.* [34] reported that alkaline etching and diffusion processes enhance the mechanical stability by approximately 11%, and that mechanical edge isolation by sawing and contact formation led to a reduction of approximately 10%–30% in the mechanical stability. With the trend to reduce the wafer thickness, the problem of overetching will be more challenging since the stability of the wafer will be reduced. If the wafers contain microcracks, the problem will be more critical and increase the breakage rate particularly where the screen printers are involved.

Another important source of microcracks is the physical stress generated during transportation [36] and handling [37], [38].

III. Classifications of Microcracks

The classification of microcracks can be based upon either the crack direction [25] or the propagation speed [26]. In this

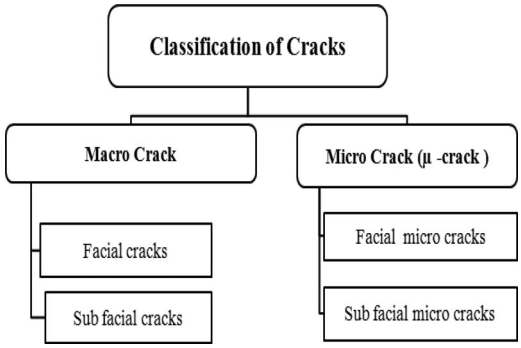

Fig. 3. Classification of cracks.

paper, we have classified cracks as either macro- or microcracks (μ-cracks) according to the crack width sizes. The crack with size smaller than 30 μm in width is usually referred to as a μ-crack [39]. The cracks are further classified according to their position as either facial or subfacial cracks. The classification scheme is shown in Fig. 3.

Cracks that occur upon the surface of a silicon wafer are referred as facial cracks. Depending on the size, it is difficult to quantify these facial cracks with the naked eye. Cracks that lie beneath the surface of a wafer or either start on the surface and propagate in the depth direction are referred to as subfacial cracks. Based upon the depth of the crack, subfacial cracks can further be classified as either deep-layer or shallow-layer cracks.

IV. Impact of the Microcracks on the Performance and Reliability of Solar Cells

Microcracks affect the electrical and mechanical properties of solar cells. Here, we discuss how these cracks affect the performance and reliability of solar cells.

A. Impact of Microcracks on the Electrical Characteristics of Solar Cells

In their study of solar cell cracking, Breitenstein *et al*. [11], [40] reported that such cracks could act as a linear or nonlinear edge shunt, and that cracks in processed solar cells led to a weak nonlinear edge recombination current, similar to nonlinear edge shunts. However, microcracks present in the starting wafer or occurring during processing prior to screen-printing metallization, may behave as severe ohmic shunts.

The faulty cell or group of cells can generate hot-spot heating problems in a module, which occurs when the operating current of a model exceeds the reduced short-circuit current of fault cell. Here, the cell is forced into reverse bias and must dissipate power. Indeed, if the dissipation power is great enough, this reverse-biased cell can overheat and melt the solder or cause deterioration of the backsheet. Hot-spot cells either exhibit low shunt resistance where the reverse-bias performance is current limited or high shunt resistance where the reverse-bias performance is voltage limited [41].

To determine the influence of the position of the cracks on the electrical parameters of the individual cells, Grunow *et al*. applied artificially varying cracks patterns to single cell modules [42]. If the cracks were parallel and centered between the bus bars, a mere power drop of less than 4% occurred. Most strikingly, however, if the cracks were parallel on both sides of both bus bars a substantial power drop of 60% occurred. Similarly, in their detailed study of microcracks, Köntges *et al*. concluded that if the location of the cracks is parallel to the bus bar, significant reduction of the module power output is observed [43], [44]. Similarly, in their study of the direct impact of microcracks on the reliability of solar cells, they observed that the power stability of the PV module is directly related to the maximum cell area that might become electrically separated. They also [45] reported the immediate effect of microcracks on the module power reduction is less than 2.5% if the crack does not hinder the electrical contact between the cell fragments.

In addition, if the solar cell with microcracks separates a part of less than 8% of the cell area, no power loss occurred. Conversely, if the inactive area of a single cell is approximately 12%–50%, the power loss increased nearly linearly from zero to the power of one double string of the PV module [45].

The unknown propagation rate for cracks in the wafer to cell metallization makes it difficult to predict the impact of the cracks on the efficiency of the PV module during its field life [46], [47]. Accelerated aging tests of PV modules with microcracks clearly indicates that cell cracks cause irregularly shaped dark regions, which reduces both the life and output of the PV module [48].

B. Impact of the Wafer Thickness on Cell Breakage in mc-Si Wafers

The fracture strength of multicrystalline silicon wafers depends upon both material-intrinsic properties (e.g., grain size, grain boundaries, and crystal orientation) and the extrinsic variables (e.g., microcracks) [49]. These surface and edge microcracks are the most important sources of degradation of mechanical strength. Reducing the potential microcracks can in turn increase the fracture strength [50]. Jorgen *et al*. [51] reported that microcracks that are located at the edge of the wafer induce breakage at lower forces than the microcracks that are located in the interior. These microcracks normally propagate along the weakest lattice directions over grains and change direction at grain boundaries. At room temperature, silicon shows elastic behavior with almost no observed plastic deformation [52]. In their study of the mechanical stability of wafers with thicknesses varying between 120 and 320 μm, Coletti *et al*. [53] reported a linear relationship between breakage force and wafer thickness. These results suggest that microcrack defects will be more critical with smaller wafer thicknesses. Although the trend is to reduce this wafer thickness, as shown in Fig. 4, the mechanical requirements necessary for that reduction will be challenging.

V. Microcrack Detection Techniques

As mentioned in Section IV, microcracks can seriously impede the solar cell performance and reliability. Because the PV industry requires a fast and precise in-line method of crack detection and characterization, many NDT techniques have been used to detect microcracks in silicon wafers and silicon solar cells. In this section, we review these NDT techniques.

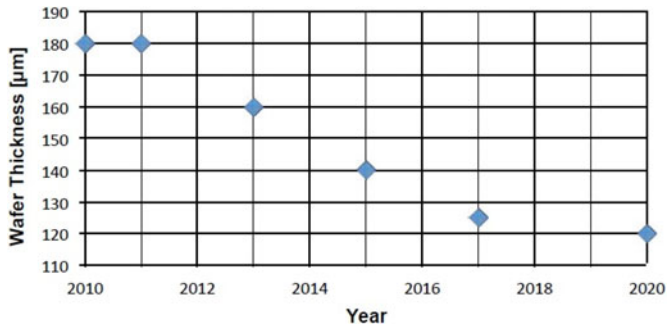

Fig. 4. Wafer thickness of previous and current generations of silicon solar cells [54].

A. Optical Transmission

In optical transmission, the silicon wafer is placed above a broad-spectrum flashlight or laser diode and the CCD camera is used to detect the optical transmission through the wafer. The microcracks inside the wafer affect the infrared portion of the light that passes through. The resolution of the CCD camera determines the minimum crack width that can be detected by this method.

Li *et al*. [55] proposed the use of a general CCD camera with a laser diode as an automatic inspection technique for facial crack detection. Although useful in detecting the facial cracks, it fails to detect hidden cracks in the awkward shaped plaques and cracks exhibiting snow-like point spread features. In addition to an infrared CCD camera and lamps behind the solar wafer, Aghamohammadi *et al*. [56] used a programmable logic controller (PLC) to acquire the signal from the computer to select a rejection line if any crack is via the image analysis system. The crack size is calculated by counting the associated dark gray pixels and the detected crack is classified based on the position of the bus bar using fuzzy logic. The advantage of this approach [56] is that it can be applied to noisy images, thus obviating the need to use preprocessing steps to filter the noise image. Rueland *et al*. [57] used the transmission of a high intensity flashlight through the wafer and high-resolution CCD camera to capture the image. A thin crack scatters the light and appears as a dark line on the image, while wider cracks let the light through the wafer and appear as white lines. The microcrack lengths are calculated by measuring the number of pixels that represent the crack. The optical transmission method is unsuitable for crack detection for finished solar cell due to the interference of the aluminum on the reverse side of the cell.

Xu *et al*. [58] used a cubic parametric spline curve to fit the cracks on the solar panel, which was useful in finding a broken edge location by using the "min" filter to obtain the gray value of cracks to note the coincident pixel location. This method has a considerably small curve fitting error compared with the least-square polynomial curve fitting. The approach of Zhuang *et al*. [59] is based on the images taken from regular visible camera, and uses image-processing techniques like gray transform, image adjustment, and contour detection. Although the microcrack is defined based upon the change in gray value of the crack pixels to the remaining pixels in the solar wafer, the visible camera and simple image-processing theory of this technique permits only the detection of elemental simple cracks. It can distinguish cracks from its surroundings only if the gray level is distinct from their surroundings.

Another technique involves the use of an LED light source (940 nm) with CCD camera to inspect and mark the position of microcracks in polycrystalline silicon wafers [60], [61]. Here, a tunable exposing system enabled the detection of microcracks even with inconstant thicknesses of the multicrystalline silicon wafer. Furthermore, once the cracks were detected, image-processing algorithms based upon histogram equalization, morphology methods, and a particles filter, were incorporated to mark the position of microcracks. Reported detection times were less than 1 s. Although the microcracks were defined as low gray level and high gradient in sensed image, this method could not discern the difference between a microcrack and a mere scratch.

Du-Ming *et al*. [62] developed a machine vision scheme to detect microcrack defects in a polycrystalline silicon wafer. The proposed method is based on anisotropic diffusion scheme, which smooths the suspected defect region and preserves the original gray levels of the faultless background patterns. The authors adjusted diffusion factors in the proposed method based on a low gray value and high gradient characteristics of a microcrack in a sensed image. Although effective in detecting cracks within 0.09 s for image size of 640×480 pixels, it could not detect subfacial cracks as it must visualize the crack on the sensed image. It also had inadequate resolution to detect such facial microcracks based on crack characteristics.

Yang [63] proposed a real-time in-line scanning method, which is based on short-time discrete wavelet transform (STDWT) to determine reflective characteristics of microcracks. Assuming the far-field condition, the operation of this system is based on the emission of a continuous pulse laser beam of 656.3 nm wavelength, through the beam is spread out by linear optics to form a line directly striking the surface of the silicon wafer. The reflected optical signal is collected by a spatial probe array and STDWT is incorporated into the post signal-processing unit. The advantage of this approach is that the entire wafer can be inspected without image-processing technology. However, the disadvantage is the tradeoff between the spatial resolution and the STDWT parameters. Although the selection of a small window size increases the spatial resolution for the proposed system, it causes an irregular pattern of the STDWT curve, making automatic identification useless.

B. Infrared Ultrasound Lock-in Thermography

Rakotoniaina *et al*. [64] used the ultrasound lock-in thermography (ULT) method to detect facial cracks in silicon wafers and solar cells. Based on the periodic introduction of ultrasound energy (USE) into the wafer, the principle of ULT is based upon the detection of heat created by friction at the edges of the crack as the USE is driven into the wafer. The USE is generated by a transducer at a fixed frequency of 20 kHz. A special resonant ultrasound coupler is used to feed-in USE into the Si wafer. Heat is detected by the infrared (IR) camera and converted into an image by the lock-in thermography (LIT) system. Using 30 min

measure time, the LIT system allows imaging of periodic surface temperature modulations having an effective value as low as 10 mK. The special resolution of this method depends on the quality of IR camera incorporated into the ULT setup. This method can detect cracks with lengths as small as 100 μm. One of the disadvantages of this technique is that the long processing time makes it unsuitable for in-line production. An additional disadvantage is that the etched cracks do not lead to local heat generation and might require covering the wafer surface with black paint, which considerably enhances the IR signal.

C. Scanning Acoustic Microscopy

Belyaev *et al*. [65] used a scanning acoustic microscope method for the detection of facial microcracks. Here, a focused high-frequency acoustic beam operating in a pulsed mode is scanned over the front surface of the wafer. These pulses are transmitted through the Si wafer at the sound velocity and are reflected at various interfaces, including the front and back surfaces of the wafer. The pulse echo technique operates at frequencies up to 250 MHz and the cracks are visualized through material discontinuity due to acoustic impedance mismatch caused by the microcracks. The time required to scan a 100 mm $\times$ 100 mm wafer, which is between 10 and 15 min, makes this method not suitable for mass production. Additionally, the wafer must be submerged in a water bath or covered with a water droplet because the high-frequency acoustic waves are attenuated quickly in air, requiring the placement of wafers in a coupling medium. However, this approach does allow the detection of cracks as small as 5–10 μm.

D. Impact Testing

In this method, the acoustic measurements are obtained by mechanically exciting vibratory modes in single-crystalline silicon wafers to detect the location and types of microcracks [66]. This method depends on the audible impact response from cracked wafer sounds, which differ from a cracked free wafer. The setup is based on applying impacts to the wafer using a miniature piezoelectric impact hammer with a vinyl tip, weight of 2.9 g and length of 10 cm and generating up to 2 000 Hz waves. The impact response is measured with a microphone mounted 2 cm above the test wafer. The reported results showed dependence of natural frequencies, peak amplitudes, and damping levels with the crack type and location. However, this approach is used in detecting only facial cracks and the force applied for the impact could initiate cracks even in crack free solar cells. Impact testing allows identification of cracks with total length of 10 mm only.

E. Resonance Ultrasonic Vibration

The resonance ultrasonic vibrations (RUV) technique developed by Belyaev *et al*. [67] is used for fast microcrack detection in solar grade crystalline silicon wafers. In this method, ultrasonic vibrations of a tunable frequency and adjustable amplitude are applied to the silicon wafer using an external piezoelectric transducer in the frequency range of 20–90 kHz. The transducer contains a central hole allowing a reliable vacuum coupling between the wafer and transducer by applying 50-kPa negative pressure to the backside of the wafer. Belyaev *et al*. [67] reported that for C-Si wafers, the increased crack length leads to decrease in peak frequency and increase in peak bandwidth. A typical RUV system can detect cracks up to submillimeter lengths. Dallas *et al*. [68] used finite-element analysis modeling to select proper vibration mode to optimize the crack detection and increase the sensitivity of the RUV technique.

F. Electronic Speckle Pattern Interferometry

Wen and Yin [69] developed a noncontact approach to detect cracks in mono- and polycrystalline solar cells using electronic speckle pattern interferometry (ESPI). In this method, speckle interference patterns are produced by real-time subtraction of sequential speckle images captured before and after an imposed deformation. This method depends on the variation of strain distribution due to thermal deformation in the solar cell, which is caused by discontinuities in material properties or the crystal lattice. A high resolution 2448 $\times$ 2050 pixels CCD camera and a DPSS laser with 532-nm wavelength are used in this method. A temperature-controllable planar heater was also used to apply a heat flux to the specimen. The ESPI image was taken from the back of the solar cells because ESPI is more suited to detect rough rather than smooth surfaces. The authors reported that under similar constraints and temperature rise, defect free specimens and specimens with microcracks shows different results [69]. This approach is used to detect both facial and subfacial cracks and can distinguish between crack and scratch.

G. Lamb Wave Air Coupled Ultrasonic Testing

Lamb wave air coupled ultrasonic testing [70], [71] is used as a noncontact rapid inspection technique to detect cracks in silicon wafers. An air-coupled transducer is used to excite and detect the antisymmetric (A0) Lamb wave mode in polycrystalline silicon wafers. The transducer is excited with an electrical spike of 900 V by a parametric pulsar/receiver with a central frequency of 200 kHz. The transmitter emits an ultrasound wave into the surrounding air, and then, enters the silicon wafer, and is converted into the Lamb wave. The Lamb wave travels through the thickness of the silicon wafer, which is captured by a receiving transducer. The reported distance between the transmitter and receiver is 100 mm. The large acoustic-impedance mismatch between the solar cell specimen and air interface, which reflects that part of that energy into the solar cell limits the usefulness of the air coupling technique, however. Depending upon the orientation of cracks, the propagation of A0 mode is blocked and the receiver will receive little or no signal compared with defect free solar cell. The proposed system is automated for crack detection with scanning time less than 15 s for each wafer. This methodology can only be used to accept or reject wafers during in-line processing because it offers rapid screening without finding the crack location. Clearly, this approach also cannot distinguish between real microcracks and other defects, since any defect could block the A0 mode.

H. Lock-in Thermography

Unlike (IR) thermography that utilizes the photon in the infrared range of the electromagnetic spectrum to produce images of a specific temperature pattern, LIT uses modulated excitation to periodically excite carriers. The sample is imaged by an IR camera running at a certain frame rate, and all images captured in a certain acquisition time are sent to the processing machine for evaluation and averaging [72], [73]. There are two main types of LIT: 1) dark lock-in thermography, and 2) illuminated lock-in thermography. The former is used by applying either a reverse bias to concentrate current in shunts or a forward bias to sense shunts and the latter uses the light instead of voltage applied by contacts to drive currents through the shunts [74], [75].

St-Laurent *et al*. [76] used IR thermography to detect subfacial microcracks. The limitation of this technique is that only cracks with shape as triangular with large mouths at the surface and tiny tips are detected. This method has not been tested to detect different shapes of microcracks and has been used only for offline inspection.

I. Electroluminescence Imaging and Photoluminescence Imaging

Luminescence results from light emissions from nonthermal energy sources. Electroluminescence (EL) imaging for solar cell characterization was introduced by Fuyuki *et al*. in 2005 [77], where the excess carriers are injected across the junction of a solar cell using an applied forward bias. The EL imaging system is a contact technique, which is only applicable for a finished solar cell.

Photoluminescence (PL) imaging is another form of luminescence that was introduced by Trupke *et al*. in 2006 [78]. PL imaging is a contactless technique with an acquisition time of typically less than 1 s used to capture luminescence images of unprocessed and partially processed wafers and finished solar cells. In the PL imaging setup, the entire surface of the sample is illuminated homogenously with an external optical energy that is equal to or greater than the semiconductor bandgap to create excess electron and hole pairs. The luminescent samples are imaged by a CCD camera with the help of an IR filter. In other words, photoluminescence is the measure of radiative recombination that depends upon the defects and impurities in the semiconductor. The photoluminescence intensity is also proportional to the carrier concentration. The photoluminescence associated with a crack is weaker due to the localized increased nonradiative recombination at crack surfaces, which makes the crack appears darker in the luminescent samples.

Both PL imaging and EL imaging systems are used for microcrack detection [79]. Breitenstein *et al*. [80] reported that the luminescence methods are better than LIT for crack inspection because luminescence imaging is usually based on an Si-detector camera that is less expensive than LIT and it does not suffer from thermal blurring, and it usually needs a lower acquisition time than LIT.

Jong-Hann *et al*. [81] developed software and hardware for an automatic optical inspection system to inspect the facial cracks of polycrystalline silicon solar cells or modules. They used the EL imaging technique with a CCD interlaced camera with 768×494 pixels resolution with optical lens mounted and illumination unit [81]. The software [81] is based on the use of a Windows-based user interface to implement the average gray level tool and the binary large object (BLOB) tool. However, it is difficult to distinguish between microcracks and other type of defects like scratches using this approach. EL equipment with a CCD camera plus lens filter has been used to capture the emissions and filter out visible spectrum for automatic detection of subfacial cracks in solar cells [82]. An image-processing scheme is used to count and recognize dark area in sensed image as microcracks. This approach cannot distinguish between the microcracks or any defects that appear as dark region in sensed EL image, however. In addition, lengthy exposure times, of about 30 s, are required. As a contact technique, the EL imaging approach can be applied only on complete solar cells and is not applicable to wafers.

Using the EL imaging system with a cooled IR camera, Tsai *et al*. [83] proposed a Fourier image reconstruction scheme to detect subfacial cracks in multicrystalline silicon solar cells. Based on the fact that the defects in the solar cell appear as line or bar shaped objects in EL image, the proposed scheme can detect defects as long as they appear darker than its surroundings in the EL image. They also reported that the defect contrast is not required to be larger than the grain boundary contrast. However, in order to have better quality results for particular cases, there should be an adaptive control approach that depends on the image parameters such as image size and resolution. They did not report the minimum microcrack size that can be detected using this approach.

The PL imaging system proposed by Yih-Chih *et al*. [39] has been used to detect invisible subfacial microcracks down to 13.4 μm. Image processing was used to extract the microcracks. The setup used a near infrared (NIR) camera with a homemade dome illuminator, which consisted of 32 pieces of 940-nm LEDs. Two different algorithms were used to extract the microcracks. The first μ-crack extraction method was based on Niblack's local segmentation algorithm [84]. The second method was based on region growing technique. The use of the second algorithm proved to be a more suitable approach for in-line applications. The sensed microcrack is assumed significantly darker than the crystal grains under infrared light. However, with this method, a dark and thin elongated crystal grain in the defect free multicrystalline silicon wafer could be falsely identified as a microcrack. Although this approach was highly accurate, the speed of inspection was low due to the low resolution of the NIR camera. The minimum detectable crack width, or the minimum detectable distance of two opposing internal microcrack surfaces is given by the wavelength of the light used in NIR. In addition, the reflection is distorted for distances smaller than the wavelength, and the minimum detectable area of the microcrack planes depend on the resolution of the digital camera. Consequently, this approach is unsuitable for detecting very slender microcracks.

TABLE I
COMPARISON OF DIFFERENT NDT TECHNIQUES

Method	Advantage	Disadvantage	References
Optical Transmission	Detect small crack ~ few μm, High Throughput ~ 1 wafer per sec, Can be used as online inspection tool	Use in production stages prior to metallization , inapplicable in finished solar cell	[55] – [63]
Infrared Lock-in Ultrasound Thermography (ULT)	Can be used both for wafers and solar cells	Long acquisition time ~ 30 minutes, might require covering the wafer surface with black paint. standalone tool	[64]
Scanning Acoustic Microscopy (SAM)	Detect cracks as small as 5–10 μm	Long acquisition time ~ 10-15 minutes, wafer has to be covered with water, used as standalone tool	[65]
Impact Testing	High Throughput	Use of impact could introduce cracks, detect cracks with total length of 10 mm only, used as standalone system	[66]
Resonance Ultrasonic Vibration (RUV)	High Throughout ~ 2 sec/ wafer. no interference with defects due to scratches	Sensitivity to crack length and crack location, used only to reject or accept wafers, does not identify the location of cracks	[67], [68]
Electronic Speckle Pattern Interferometry (ESPI)	No interference with defects due to scratches	Resolution to measure the crack length is 2.65 mm for 25 mm long crack.	[69]
Lamb Wave Air Coupled Ultrasonic Testing (LAC-UT)	Scanning time < 15 sec/ wafer, ability to quantify the cracks in terms of length	Only used for accepting or rejecting wafers during online processing, can't distinguish between real crack and any defect could block the A0 mode.	[70], [71]
Lock-in Thermography (LIT)	High resolution imaging of defects	Offline inspection only, long acquisition time, suffer from thermal blurring	[72]-[76]
Electroluminescence (EL) imaging	High Throughput	Interference with other defects (e.g. scratches), contacted method , can be used only with finished solar cell, standalone system	[77], [79], [80]-[83]
Photoluminescence (PL) imaging	High Throughput, contactless can be used as online inspection tool for both wafers and solar cells	Interference with other defects such as scratches	[78], [79], [39]

VI. COMPARISON OF MICROCRACK DETECTION TECHNIQUES

Microcracks adversely affect the manufacturing cost and reliability of PV modules. In Table I, we have compared the weakness and strength of different NDT techniques to detect microcracks in mono- and polycrystalline silicon wafers and solar cells. As we have discussed in the previous section, there are many types of inspection tools used to detect microcracks. If

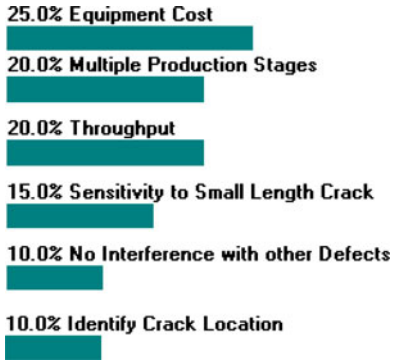

Fig. 5. Proposed criteria and relative weight used in this study.

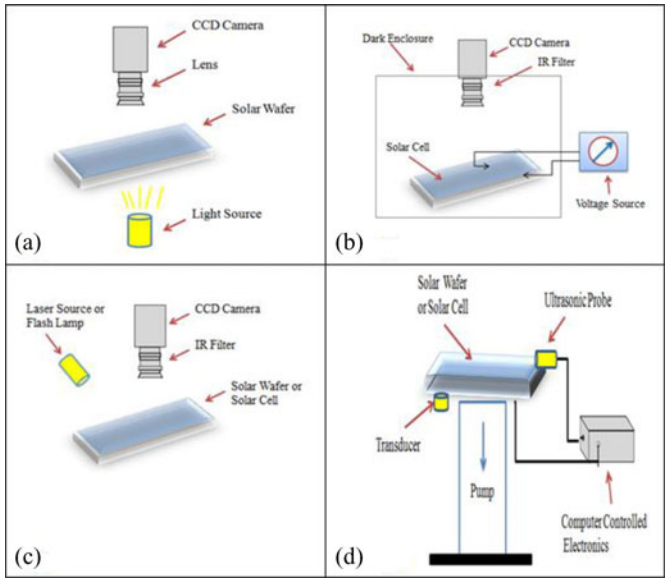

Fig. 6. Alternatives are based on (a) optical transmission, (b) EL imaging, (c) PL imaging, and (d) RUV.

the production line is fully automated, the inspection tools must be fast and precise. Only tools that are based on PL imaging, EL imaging, optical transmission, and RUV meet these requirements. However, if there is a need to detect microcracks only in the finished solar cell stage, we can use an inspection tool that is based only on EL imaging and not tools that are based on optical transmission. Should an inspection tool be required during the wafer and finished solar cell manufacturing stages, we can use PL imaging or RUV-based inspection tools. Some commercial inspection tools that use PL imaging technology, such as that created by the BT Imaging Company formed by Bardos and Trupke [85], provide many products for inline inspection tools for both wafer and solar cells. The throughput for this tool is up to 3600 measurements per hour where the throughput for the commercial RUV system [86] is between 1200–1800 measurements per hour. There are many methods for microcrack inspections, each of which has their advantages and disadvantages. In the following section, we describe, for the first time, our use of a methodology to rank these various microcrack inspection tools.

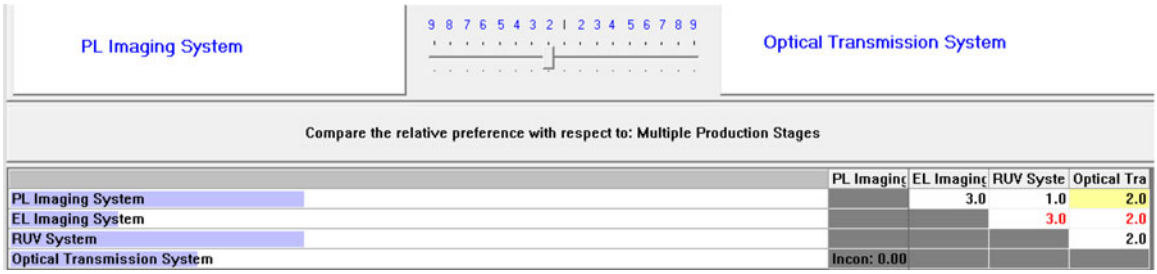

Fig. 7. Pairwise comparison between main selection criteria.

VII. Nondestructive Testing Tool Selection Study

Our objective is to rank the different crack detection tools reviewed in this paper for a specific PV production line. Our decision-making tool is based on the AHP to rank different inspection tools based on given selection criteria. The AHP [87] provides a comprehensive framework for structuring a system of objectives, criteria and alternatives. The AHP hierarchy is used to establish a relation in the first hierarchy level between objective function and between criteria and alternatives in the second hierarchy level. The AHP is used in a number of decision-making applications, e.g., Byun [88] used AHP to provide a structure on decision-making for car purchase. Bhattacharyay *et al*. [89] used AHP for robot selection. In addition, two of the current authors used AHP to assist in the material selection for the automotive body-in-white (BiW) panels at the conceptual design stage [90] and for automotive production line design [91].

Our proposed approach for using AHP is based on the following specifications.

1) The ultimate goal is to choose best microcrack detection tool for specific mono- and polycrystalline PV production line. This is the first level in AHP.
2) The second level in AHP, known as criteria, is dependent upon the requirements of a specific production line. We assume that the specific production line requires an inspection tool, which can work on multiple production stages (wafer and cell), with high throughput and can be incorporated into a fully automated PV production line. Initial equipment cost is perhaps the highest priority, followed by the sensitivity to discern small crack length. The inspection tool must also be precise in identifying microcracks without any concern of false detection. Fig. 5 shows the criteria with relative weight, where the highest priority criterion has the highest weight and the total weights for all criterions is equal 100%.
3) The third level of hierarchy, known as alternatives or competitors, represents the four inspection tools. Fig. 6 shows the setup for the alternatives.
4) The relation between each criterion and each alternative in the second hierarchy level is established by a pairwise comparison between two elements simultaneously. For each criterion, i.e., multiple production stages, we compare between two alternatives at a time. For example, we start with a comparison between PL and EL imaging systems. After comparing the alternatives, it should be repeated for different criterion using the same procedure.

   Fig. 7 shows pairwise comparisons between PL imaging and optical transmission based on multiple production stages. As displayed in Fig. 7, the result of this comparison is equal to 2, which implies that the ratio between the PL imaging systems to optical transmission is equal to 2:1. Our calculations in this step are based on Table I, which is the summary of the literature data presented in this study. The PL imaging system is capable of detecting microcracks in unprocessed and partially processed wafers and finished solar cells, but the optical transmission can detect microcracks only in the production stages prior to metallization. Since it is inapplicable for finished solar cells, it results in a ratio of 2:1. If the comparison is between PL imaging and EL imaging for use in a multiple production stages criterion, the ratio will be 3:1 since EL imaging is only applicable for the inspection of finished solar cells.
5) The final step is to rank all the alternatives (microcrack inspection tools) based upon the overall criteria (production line requirements) to satisfy the ultimate goal of selecting the best microcrack detection tool. The results shown in Fig. 8 indicate that the PL imaging system is the best system, with a 27.3% rate of effectiveness, making it the best for this production line. The second ranked system is the optical transmission system followed by the RUV system in third place. An EL imaging system is the last ranked tool.

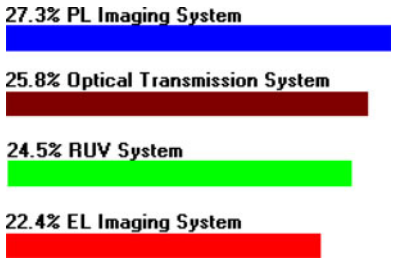

Fig. 8. Rank of the selection alternatives with respect to goal statement.

Fig. 9 shows the rank for all alternatives based on each of the selection criterion and shows the sensitivity for different constraints with respect to the ultimate goal. Fig. 9 also shows the values for each alternative with regard to each constraint. As shown in Fig. 9, the problem has conflicting objectives and

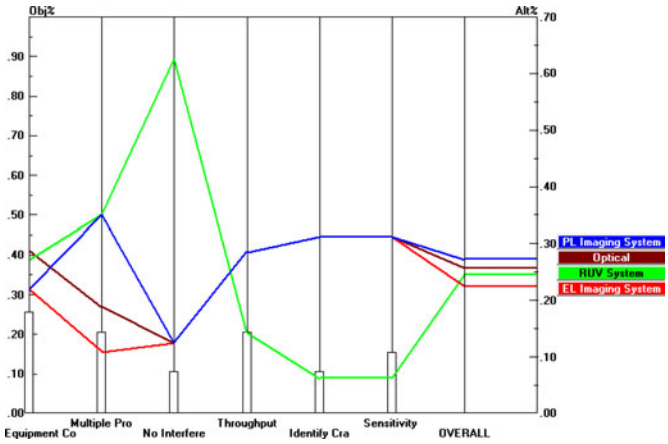

Fig. 9. Sensitivity for different constraint with respect to the ultimate goal.

multi-attribute constraints (e.g., no interference with other defects criterion, RUV system has the best rank, but has the lowest rank as regards to throughput).

VIII. Conclusion

In this paper, we reviewed the origin and root causes of microcracks in mono- and polycrystalline silicon wafers and solar cells, and the strengths and weaknesses of various nondestructive techniques used for the detection of microcracks. For automated manufacturing plants, the optimum microcrack detection techniques must satisfy conflicting objectives and multi-attribute constraints. We used a decision-making tool that is based on the AHP to rank various inspection tools based upon specific criteria. Our results indicate that the microcrack detection system based upon the PL imaging system was superior to all others and ideally suited for automated production lines.

References

[1] J. Montgomery. (2013, Feb. 12). 100 GW of Solar PV Now Installed in the World Today. [Online]. Available: http://www.renewableenergyworld.com/rea/news/article/2013/02/100-gw-of-solar-pv-now-installed-in-the-world-today

[2] S. Clara. (2013, Mar. 11). Solar Photovoltaic Demand to Reach 31 Gigawatts in 2013: According to NPD Solarbuzz. [Online]. Available: http://www.prweb.com/releases/2013/3/prweb10514041.htm

[3] S. Staff. (2013, May 21). Global Solar PV Market Poised to 'Rise From the Ashes' Of 2011. [Online]. Available: http://www.solarindustrymag.com/e107_plugins/content/content.php?content.12701

[4] R. Singh and G. F. Alapatt. (2012, Oct. 11). Innovative paths for providing green energy for sustainable global economic growth. *Proc. SPIE, Photon. Innovations Solutions Complex Environ. Syst.* [Online]. vol. 8482, p. 848205. Avaliable:http://dx.doi.org/10.1117/12.928058

[5] P. Mints. (2013, Mar. 20). Solar PV Profit's Last Stand. [Online]. Available: http://www.renewableenergyworld.com/rea/news/article/2013/03/solar-pv-profits-last-stand?cmpid=SolarNL-2013-03-22

[6] Z. Shahan. (2013, May 11). Solar Module Manufacturing Trends in 2012. [Online]. Available: http://cleantechnica.com/2013/05/11/solar-module-manufacturing-trends-in-2012/

[7] R. Singh, "Why silicon is and will remain the dominant photovoltaic material," *J. Nanophoton.*, vol. 3, no. 1, pp. 032503–032513, 2009, doi: 10.1117/1.3196882.

[8] J. M. Martimez-Duart and J. Hernandez-Moro, "Commentary: Photovoltaics firmly moving to the terawatt scale," *J. Nanophoton.*, vol. 7, no. 1, pp. 078599–078602, Mar. 22, 2013, doi:10.1117/1.JNP.7.078599.

[9] M. Green, K. Emery, Y. Hishikawa, W. Warta, and E. Dunlop, "Solar cell efficiency tables (Version 40)," *Progr. Photovolt., Res. Appl.*, vol. 20, pp. 606–614, 2012.

[10] SunPower® Residential Solar Panels. (2013). [Online]. Available: http://us.sunpowercorp.com/homes/products-services/solar-panels/

[11] O. Breitenstein, J. P. Rakotoniaina, M. H. AI Rifai MH, and M. Werner, "Shunt types in crystalline silicon solar cells," *Progr. Photovolt., Res. Appl.*, vol. 12, pp. 529–538, 2004.

[12] S. A. Correia, J. Lossen, and M. Bahr, "Eliminating shunts from industrial silicon solar cells by spatially resolved analysis," in *Proc. 21st Eur. Photovolt. Sol. Energy Conf.*, 2006, pp. 1297–1300.

[13] O. Breitenstein, J. Bauer, and J. P. Rakotoniaina, "Material-induced shunts in multicrystalline silicon solar cells," *J. Semicond.*, vol. 41, no. 4, pp. 440–443, 2007.

[14] Z. Lucheng, X. Xinxiang, Y. Zhuojian, S. Xiaopu, X. Hongyun, L. Haobin, and S. Hui, "An efficient method for monitoring the shunts in silicon solar cells during fabrication processes with infrared imaging," *J. Semicond.*, vol. 30, no. 7, pp. 076001–076004, 2009.

[15] G. Acciani, O. Falcone, and S. Vergura, "Typical defects of PV-cells," in *Proc. Int. Symp. Ind. Electron. Conf.*, 2010, pp. 2745–2749.

[16] J. Rakotoniaina, S. Neve, M. Werner, and O. Breitenstein, "Material induced shunts in multicrystalline silicon solar cells," in *Proc. Conf. Photovolt. Eur.*, Rome, Italy, 2002, pp. 24–27.

[17] M. Kusko, M. Perný, and V. Šály, "Dark and under illumination electric PV parameters of modified solar cells," *ELEKTROENERGETIKA*, vol. 4, no. 2, pp. 5–7, 2011.

[18] B. Gao, S. Nakano, and K. Kakimoto, "Effect of crucible cover material on impurities of multicrystalline silicon in a unidirectional solidification furnace," *J. Crystal Growth*, vol. 318, pp. 255–258, 2011.

[19] S. Riepe, I. E. Reis, W. Kwapil, M. A. Falkenberg, J. Schön, H. Behnken, J. Bauer, D. Kreßner-Kiel, W. Seifert, and W. Koch, "Research on efficiency limiting defects and defect engineering in silicon solar cells – results of the German research cluster Solar Focus," *Phys. Status Solidi C*, vol. 8, no. 3, pp. 733–738, 2011.

[20] A. Schieferdecker, J. Sachse, T. Mueller, U. Seidel, L. Bartholomaeus, S. Germershausen, R. Perras, R. Meissner, H. Hoebbel, A. Schenke, K. Bhatti, K. H. Küsters, and H. Richter, "Material effects in manufacturing of silicon based solar cells and modules," *Phys. Status Solidi C*, vol. 8, no. 3, pp. 871–874, 2011.

[21] P. Rupnowski and B. Sopori, "Strength of silicon wafers: Fracture mechanics approach," *Int. J. Fracture*, vol. 155, no. 1, pp. 67–74, 2009.

[22] S. Wansleben. (2011, Mar.). Not Falling Through the Crack. [Online]. Available: http://www.pv-magazine.com/archive/articles/beitrag/not-falling-through-the-cracks_100002343/#ixzz2XlDuI4Bt

[23] M. Israil, S. A. Anwar, and M. Z. Abdullah, "Automatic detection of micro-crack in solar wafers and cells: A review," *Trans. Inst. Meas. Control*, vol. 35, no. 5, pp. 606–618, Jul. 2013.

[24] B. Lawn, *Fracture in Brittle Solids*, 2nd ed. Cambridge, U.K.: Cambridge Univ. Press, 1975.

[25] R. Perez and P. Gumbsch, "Directional anisotropy in the cleavage fracture of silicon," *Phys. Rev. Lett.*, vol. 84, no. 23, pp. 5347–5350, 2000.

[26] J. Hauch, D. Holland, M. P. Marder, and H. L. Swinney, "Dynamic fracture in single crystal silicon," *Phys. Rev. Lett.*, vol. 82, no. 19, pp. 3823–3826, 1999.

[27] M. J. Buehler, H. Tang, C. T. Adri, V. Duin, and W. A. Goddard, "Threshold crack speed controls dynamical fracture of silicon single crystals," *Phys. Rev. Lett.*, vol. 99, pp. 165502–165505, 2007, doi: 10.1103/PhysRevLett.99.165502.

[28] M. F. Hafiz and T. Kobayashi, "Fracture toughness of eutectic Al–Si casting alloy with different microstructural features," *J. Mater. Sci.*, vol. 31, pp. 6195–6200, 1996.

[29] I. Chasiotis, S. W. Cho, and K. Jonnalagadda, "Fracture toughness and subcritical crack growth in polycrystalline silicon," *J. Appl. Mech.*, vol. 73, pp. 714–722, 2006.

[30] L. Johnsen, T. Bergstrom, M. M'Hamdi, and K. Kay Gastinger, "The importance of temperature control during crystallization and wafering in silicon solar cell," in *Photovoltaics International*, 7th ed., Feb. 2010, pp. 49–54.

[31] Y. K. Park, M. C. Wagener, N. Stoddard, M. Bennett, and G. A. Rozgonyi GA, "Correlation between wafer fracture and saw damage introduced during cast silicon cutting," in *Proc. 15th Workshop Crystalline Silicon Sol. Cells Modules, Mater. Processes*, Vail, CO, USA, Aug. 7–10, 2005, pp. 178–181.

[32] H. Park, S. Kwon, J. SungLee, H. Lim, S. Yoon, and D. Kim, "Improvement on surface texturing of single crystalline silicon for solar cells by

saw-damage etching using an acidic solution," *Sol. Energy Mater. Sol. Cells*, vol. 93, pp. 1773–1778, 2009.
[33] H. Larsson, J. Gustafsson, H. J. Solheim, and T. Boström, "The impact of saw damage etching on microcracks in solar cell production," presented at the 23rd Eur. Photovoltaics Solar Energy Conf., Valencia, Spain, 2008.
[34] A. Schneider, G. Bühler, F. Huster, K. Peter, and P. Fath, "Impact of individual process steps on the stability of silicon solar cells studied with a simple mechanical stability tester," presented at the PV in Europe from PV Technology to Energy Solutions Conf., Rome, Italy, 2002.
[35] T. Geipel, S. Pingel, J. Dittrich, Y. Zemen, G. Kropke, M. Wittner, and J. Berghold, "Comparison of acidic and alkaline textured multicrystalline solar cells in a solar panel production," in *Proc. 24th Eur. Photovolt. Sol. Energy Conf.*, Hamburg, Germany, Sep. 21–25, 2009, pp. 3248–3252.
[36] M. Köntges, S. Kajari-Schröder, I. Kunze, and U. Jahn, "Crack statistic of crystalline silicon photovoltaic modules," presented at the 26th Eur. Photovoltaic Solar Energy Conf. Exhib., Hamburg, Germany, Sep. 5–6, 2011.
[37] X. F. Brun and S. N. Melkote, "Analysis of stresses and breakage of crystalline silicon wafers during handling and transport," *Sol. Energy Mater. Sol. Cells*, vol. 93, pp. 1238–1247, 2009.
[38] M. Sander, B. Henke, S. Schweizer, M. Ebert, and J. Bagdahn, "PV module defect detection by combination of mechanical and electrical analysis methods," presented at the IEEE 35th Photovoltaic Specialists Conf., Honolulu, HI, USA, Jun. 20–25, 2010.
[39] Y. Chiou and J. Liu J, "Micro crack detection of multi-crystalline silicon solar wafer using machine vision techniques," *Sensor Rev.*, vol. 31, no. 2, pp. 154–165, 2011.
[40] O. Breitenstein, J. Bauer, P. P. Altermatt, and K. Ramspeck, "Influence of defects on solar cell characteristics," *Solid State Phenom.*, vol. 156–158, pp. 1–10, 2010.
[41] J. Wohlgemuth and W. Herrmann, "Hot spot tests for crystalline silicon modules," in *Proc. IEEE 31st Photovolt. Spec. Conf. Rec.*, Jan. 3–7, 2005, pp. 1062–1063.
[42] P. Grunow, P. Clemens, V. Hoffmann, B. Litzenburger, and L. Podlowski, "Influence of micro cracks in multi-crystalline silicon solar cells on the reliability of PV modules," presented at the 20th Eur. Photovoltaic Solar Energy Conf., Barcelona, Spain, Jun. 6–10, 2005.
[43] M. Köntges, S. Kajari-Schröder, I. Kunze, and U. Jahn, "crack statistic of crystalline silicon photovoltaic modules," presented at the 26th Eur. Photovoltaic Solar Energy Conf. Exhib., Hamburg, Germany, Sep. 5–6, 2011.
[44] S. Kajari-Schroder, I. Kunze, U. Eitner, and M. Kontges, "Spatial and orientational distribution of cracks in crystalline photovoltaic modules generated by mechanical load tests," *Sol. Energy Mater. Sol. Cells*, vol. 95, pp. 3054–3059, 2011.
[45] M. Köntges, S. Kajari-Schröder, I. Kunze, and U. Jahn U, "The risk of power loss in crystalline silicon based photovoltaic modules due to micro-cracks," *Sol. Energy Mater. Sol. Cells*, vol. 95, pp. 1131–1137, 2011.
[46] S. Pingel, Y. Zemen, O. Frank, T. Geipel, and J. Berghold, "Mechanical stability of solar cells within solar panels," in *Proc. 24th Eur. Photovolt. Sol. Energy Conf.*, Dresden, Germany, 2009, pp. 3459–3464.
[47] A. M. Gabor, M. M. Ralli, L. Alegria, C. Brodonaro, J. Woods, and L. Felton, "Soldering induced damage to thin Si solar cells and detection of cracked cells in modules," in *Proc. 21st Eur. Photovolt. Sol. Energy Conf*, Dresden, Germany, 2006, pp. 2042–2047.
[48] P. Chaturvedi, B. Hoex, and T. M. Walsh. (2013). "Broken metal fingers in silicon wafer solar cells and PV modules," *Sol. Energy Mater. Sol. Cells*, vol. 108, pp. 78–81. [Online]. Available: http://dx.doi.org/10.1016/j.solmat.2012.09.013
[49] V. A. Popovich, T. Amstel, I. J. Bennett, M. Janssen, and I. M. Richardson, "Microstructure and mechanical properties of aluminum back contact layers," presented at the 24th Eur. Photovoltaic Solar Energy Conf., Hamburg, Germany, 2009.
[50] V. A. Popovich, A. Yunus, M. Janssen, I. J. Bennett, and I. M. Richardson, "Effect of silicon solar cell processing parameters and crystallinity on mechanical strength," *Sol. Energy Mater. Sol. Cells*, vol. 95, pp. 97–100, 2011.
[51] J. Gustafsson, H. Larsson, H. J. Solheim, and T. Boström, "Mechanical stress tests on Mc-Si wafers with microcracks," presented at the 23rd Eur. Photovoltaic Solar Energy Conf., Valencia, Spain, 2008.
[52] G. Coletti, C. J. Tool, and L. J. Geerligs, "Mechanical strength of silicon wafers and its modeling," in *Proc. 15th Workshop Crystalline Silicon Sol. Cells Modules, Mater. Processes*, Vail, CO, USA, Aug. 7–10, 2005, pp. 117–20.
[53] G. Coletti, V. D. Borg, S. D. Iuliis, C. J. Tool, and L. J. Geerligs, "Mechanical strength of silicon wafers depending on wafer thickness and surface treatment," presented at the 21st Eur. Photovoltaic Solar Energy Conf. Exhib., Dresden, Germany, Sep. 4–8, 2006.
[54] M. Fischer. (2012, Mar.). International Technology Roadmap for Photovoltaic (ITRPV)—3rd Edition—Results 2011. [Online]. Available: http://www.semi.org/eu/sites/semi.org/files/docs/05PVFMF2012_Markus%20Fischer_Q-Cells_ITRPV-Results_2011.pdf
[55] B. Li, H. Xianghao, and F. Shuai, "Automatic inspection of surface crack in solar cell images," in *Proc. Chin. Control Decision Conf.*, 2011, pp. 993–998.
[56] A. H. Aghamohammadi, A. S. Prabuwono, S. Sahran, and M. Mogharrebi, "Solar cell panel crack detection using particle swarm optimization algorithm," in *Proc. Int. Conf. Pattern Anal. Intell. Robot.*, Putrajaya, Malaysia, Jun. 28–29, 2011, pp. 160–164.
[57] E. Rueland, A. Herguth, A. Trummer, S. Wansleben, and P. Fath, "Microcrack detection an other optical characterization techniques for in-line inspection of wafers and cells," in *Proc. 20th Eur. Photovoltaic Solar Energy Conf.*, Barcelona, Spain, 2005, pp. 3242–3245.
[58] M. Xu, H. Wang, and Z. Gui, "Solar panel surface crack extraction using curve fitting," in *Proc. 2nd Int. Conf. Educ. Technol. Comput.*, 2010, vol. 3, pp. 90–94.
[59] F. Zhuang, Z. Yanzheng, L. Yang, C. Qixin, C. Mingbo, Z. Jun, and J. Lee, "Solar cell crack inspection by image processing," in *Proc. Int. Business Electron. Product Rel. Liability Conf.*, Apr. 27–30, 2004, pp. 77–80.
[60] S. Ke, K. Lin, Y. Lin, J. Chen, Y. Wang, and C. Liu, "High-performance inspecting system for detecting micro-crack defects of solar wafer," in *Proc. IEEE Sensors Conf.*, Nov. 1–4, 2010, pp. 494–497.
[61] S. Ko, C. Liu, and Y. Lin. (2013, Mar.). Optical inspection system with tunable exposure unit for micro-crack detection in solar wafers. *Optik–Int. J. Light Electron Opt.* [Online]. Available: http://dx.doi.org/10.1016/j.ijleo.2012.12.024
[62] D. Tsai, C. Chang, and S. Chao, "Micro-crack inspection in heterogeneously textured solar wafers using anisotropic diffusion," *Image Vis. Comput.*, vol. 28, no. 3, pp. 491–501, 2010.
[63] W. Yang, "Short-time discrete wavelet transform for wafer microcrack detection," in *Proc. IEEE Int. Symp. Ind. Electron.*, Seoul, Korea, Jul. 5–8, 2009, pp. 2069–2074.
[64] J. P. Rakotoniaina, O. Breitenstein, M. H. Al Rifai, D. Franke, and A. Schnieder, "Detection of cracks in silicon wafers and solar cells by lock-in ultrasound thermography," in *Proc. PV Sol. Conf.*, Paris, France, 2004, pp. 640–643.
[65] A. Belyaev, O. Polupan, S. Ostapenko, D. P. Hess, and J. P. Kalejs, "Resonance ultrasonic vibration diagnostics of elastic stress in full-size silicon wafers," *Semicond. Sci. Technol.*, vol. 21, pp. 254–260, 2006.
[66] C. Hilmersson, D. P. Hess, and W. Dallas, "Crack detection in single-crystalline silicon wafers using impact testing," *Appl. Acoust.*, vol. 69, no. 8, pp. 755–760, 2008.
[67] A. Belyaev, O. Polupan, W. Dallas, S. Ostapenko, D. Hess, and J. Wohlgemuth, "Crack detection and analyses using resonance ultrasonic vibrations in full-size crystalline silicon wafers," *Appl. Phys. Lett.*, vol. 88, no. 11, pp. 111907–111909, 2006, doi: 10.1063/1.2186393.
[68] W. Dallas, O. Polupan, and S. Ostapenko, "Resonance ultrasonic vibrations for crack detection in photovoltaic silicon wafers," *Meas. Sci. Technol.*, vol. 18, pp. 852–858, 2007.
[69] T. Wen and C. Yin, "Crack detection in photovoltaic cells by interferometric analysis of electronic speckle patterns," *J. Sol. Energy Mater. Sol. Cells*, vol. 98, pp. 216–223, 2012.
[70] S. K. Chakrapani, M. J. Padiyar, and K. Balasubramaniam, "Crack detection in full size cz-silicon wafers using lambwave air coupled ultrasonic testing (LAC-UT)," *J. Nondestructive Eval.*, vol. 31, pp. 46–55, 2012.
[71] M. J. Padiyar, S. K. Chakrapani, C. V. Krishnamurthy, and K. Balasubramaniam, "Crack detection in polycrystalline silicon wafers using air-coupled ultrasonic guided waves," in *Proc. Nat. Seminar Exhib. Non-Destructive Eval.*, Dec. 10–12, 2009, pp. 341–345.
[72] O. Breitenstein, M. Langenkamp, O. Lang, and A. Schirrmacher, "A. shunts due to laser scribing of solar cell evaluated by highly sensitive lock-in thermography," *Sol. Energy Mater. Sol. Cells*, vol. 65, no. 1, pp. 55–62, 2001.
[73] O. Breitenstein and M. Langenkamp, *Lock-in Thermography—Basics and Use for Functional Diagnostics of Electronic Components*. Berlin, Germany: Springer, 2003.
[74] Lock-in Thermography Imaging Workstation. (2012). [Online]. Available: http://www.nrel.gov/pv/pdil/samc_thermography.html

[75] O. Breitenstein, "Illuminated versus dark lock-in thermography investigations of solar cells," *Int. J. Nanoparticles*, vol. 6, no. 2/3, pp. 81–92, 2013.
[76] L. St-Laurent, M. Genest, C. Simon, and X. Maldague, "Micro-cracks detection in photo-voltaic cells by infrared thermography," presented at the 7th Int. Conf. Quantitative Infrared Thermography, Brussels, Belgium, Jul. 5–8, 2004.
[77] T. Fuyuki, H. Kondo, T. Yamazaki, Y. Takahashi, and Y. Uraoka, "Photographic surveying of minority carrier diffusion length in polycrystalline silicon solar cells by electroluminescence," *Appl. Phys. Lett.*, vol. 86, no. 26, pp. 262108–262110, 2005, doi: 10.1063/1.1978979.
[78] T. Trupke, R. A. Bardos, M.C. Schubert, and W. Warta, "Photoluminescence imaging of silicon wafers," *Appl. Phys. Lett.*, vol. 89, no. 4, pp. 044107–044107–3, Jul. 2006.
[79] T. Trupke, R. A. Bardos, M. D. Abbott, P. Würfel, E. Pink, Y. Augarten, F. W. Chen, K. Fisher, J. E. Cotter, M. Kasemann, M. Rüdiger, S. Kontermann, M. C. Schubert, M. The, S. W. Glunz, W. Warta, D. Macdonald, J. Tan, A. Cuevas, J. Bauer, R. Gupta, O. Breitenstein, T. Buonassisi, G. Tarnowski, A. M. Lorenz, H. P. Hartmann, D. H. Neuhaus, and J. M. Fernandez, "Progress with luminescence imaging for the characterisation of silicon wafers and solar cells," presented at the 22nd European Photovoltaic Solar Energy Conference, Milan, Italy, Sep. 3–7, 2007.
[80] O. Breitenstein, J. Bauer, K. Bothe, D. Hinken, J. Muller, W. Kwapil, M. C. Schubert, and W. Warta, "Can luminescence imaging replace lock-in thermography on solar cells," *IEEE J. Photovolt.*, vol. 1, no. 2, pp. 159–167, Oct. 2011.
[81] J. Jean, C. Chen, and H. Lin, "Application of an image processing software tool to crack inspection of crystalline silicon solar cells," presented at the 2011 Int. Conf. Machine Learning and Cybernetics, Guilin, China, Jul. 2011.
[82] W. J. Lin, Y. H. Lei, and C. H. Huang, "Automatic detection of internal defects in solar cells," in *Proc. Instrum. Meas. Technol. Conf.*, Binjiang, China, May 10–12, 2011, pp. 1–4.
[83] D. M. Tsai, S. C. Wu, and W. C. Li, "Defect detection of solar cells in electroluminescence images using Fourier image reconstruction," *Sol. Energy Mater. Sol. Cells*, vol. 99, pp. 250–262, 2012.
[84] W. Niblack, *An Introduction to Digital Image Processing*. Englewood Cliffs, NJ, USA: Prentice Hall, 1986, pp. 115–116.
[85] BT Imaging. (2008). [Online]. Available: http://www.btimaging.com/
[86] RUV Systems. (2009). [Online]. Available: http://www.ruvsystems.nl/
[87] T. L. Saaty, *Decision Making with Feedback: The Analytical Network Process*. Pittsburg, PA, USA: RWS, 1996.
[88] D. H. Byun, "The AHP approach for selecting an automobile purchase model," *Inform. Manage.*, vol. 38, pp. 289–297, 2001.
[89] A. Bhattacharyay, B. Sarkar, and S. Mukherjee, "Integrating AHP with QFD for robot selection under requirement perspective," *Int. J. Prod. Res.*, vol. 43, no. 17, pp. 3671–3685, 2005.
[90] A. Mayyas, Q. Shen, A. Mayyas, M. Abdelhamid, D. Shan, A. Qattawi, and M. Omar, "Using quality function deployment and analytical hierarchy process for material selection of body-in-white," *Mater. Design*, vol. 32, pp. 2771–2782, 2011.
[91] A. Qattawi, A. Mayyas, M. Abdelhamid, and M. Omar, "Incorporating quality function deployment and analytical hierarchy process in a knowledge-based system for automotive production line design," *Int. J. Comput. Integr. Manuf.*, vol. 26, no. 9, pp. 839–856, 2013.

Mahmoud Abdelhamid (S'12) received the B.S. degree in electrical and computer engineering from Hashemite University, Zarqa, Jordan, in 2004 and the M.S. degree in mechanical engineering from Clemson University, Clemson, SC, USA, in 2011, in the area of Autonomous Pick & Place using a robotic manipulator. He is currently working toward the Ph.D. degree with the Clemson University International Center for Automotive Research, Clemson, SC, USA.

His research has been published as a one-book manuscript, as well as in several journal publications and conference proceedings. His research interests include the area of nondestructive testing of materials, photovoltaic solar cells, and decision making tools for automotive applications. His current research work is focused on the process of photovoltaic solar cells for vehicle applications.

Rajendra Singh (S'75–M'78–SM'82–F'02) received the Ph.D. degree in physics from McMaster University, Hamilton, ON, Canada, in 1979.

He is currently a D. Houser Banks Professor with the Holcombe Department of Electrical and Computer Engineering and the Director of the Center for Silicon Nanoelectronics, Clemson University, Clemson, SC, USA. With proven success in operations, project/program leadership, R&D, product/process commercialization, and start-ups, he is a leading semiconductor and photovoltaic (PV) Expert with more than 34 years of industrial and academic experience of photovoltaic and semiconductor industries. The technology invented by him at Energy Conversion Devices is used in the manufacturing of amorphous thin film PV modules. The technology invented by him has been licensed to RTP tool manufacturer AG Associates. From solar cells to integrated circuits, he has led the work on semiconductor and photovoltaic device materials and processing by manufacturable innovation and defining critical path. He has published more than 370 papers in various journals and conference proceedings.

Dr. Singh is an Editor or a Co-editor of more than 15 conference proceedings. He has presented more than 50 keynote addresses and invited talks in various national and international conferences. He has served on a number of committees of various professional societies. He is currently the Chair of the IEEE Electron Devices Society Technical Committee on Semiconductor Manufacturing and an Editor of the IEEE JOURNAL OF ELECTRON DEVICES SOCIETY. He has received the IEEE Distinguished Lecturer for Latin American on Solar Cells (Region 9) Award (1983), the Distinguished Technologist United Nations Development Program Award (1987), the IEEE Electron Device Society Distinguished Lecturer Award (1994–2012), the Outstanding Researcher Award Sigma Xi Chapter, Clemson University (1997), five Clemson University awards for Faculty Excellence, the Thomas D. Callinan Award of the Electrochemical Society (1998), the J.F. Gibbons Award from the 11th IEEE International Conference on Advanced Thermal Processing of Semiconductors (2003), and the 2005 McMaster University Distinguished Alumni Award. Photovoltaics World (October 2010) selected him as one of the ten Global "Champions of Photovoltaic Technology." He is Fellow of the Society of Optical Engineering, American Association for the Advancement of Science, and the American Society of Metals.

Mohammed Omar received the B.S degree in mechanical engineering from Jordan University, Amman, Jordan, in 2001 and the Ph.D. degree from the University of Kentucky, Lexington, KY, USA, in 2005.

He has served as a Visiting Scholar with the Toyota Motor Company Measurement and Instrumentation Engineering Division, in addition to serving as a Postdoctoral Scholar with the University of Kentucky Center for Manufacturing. Currently, he is an Associate Professor with the Clemson University International Center for Automotive Research. His research and teaching interests include the areas of manufacturing and materials and design; specifically, knowledge-based manufacturing systems and light-weight design, and nondestructive testing of materials and structures. His research has been published in four book manuscripts and more than 100 journal publications and conference proceedings. He holds four international and US patents.

Dr. Omar is currently the Editor-in-Chief for the *Journal of Material Science Research.*